

Quantitative Image and Data Analysis – Mapping Quantitative Parameters

Gareth .J. Barker
King's College London,
Institute of Psychiatry, Department of Clinical Neuroscience,
Centre for Neuroimaging Sciences,
De Crespigny Park, London, SE5 8AF, UK

Introduction

Signal intensity from most MR pulse sequences does NOT relate directly to any single physical parameter; all sequences have signal which is proportional to proton density, PD, and scaled by an arbitrary gain which is scanner, session and object dependant. One exception is SSFP (Steady State Free Precession) (also known as FISP - Fast Imaging with Steady-state Precession), for which the signal intensity is given by

$$I_{GE} \approx \frac{gPD \sin(\alpha)}{\left[1 + \frac{T_1}{T_2} - \cos(\alpha)\left(\frac{T_1}{T_2} - 1\right)\right]}$$

For flip angle, α , = 90° this reduces to a function of the relaxation times, T_1 and T_2 , only:

$$I_{GE} \propto \frac{T_2}{[T_1 + T_2]} \approx \frac{T_2}{T_1}$$

Calculating quantitative parameters, rather than relying on interpretation of the MR images themselves, can potentially increased sensitivity to changes associated with disease. It allows quantitative, not qualitative, assessment, with values being compared to normal ranges, and should also make results less scanner independent, making longitudinal or multi-centre studies much easier.

There are a number of parameters that can be quantified by MR, the most commonly investigated being T_1 , T_2 , magnetisation transfer related parameters (ranging from the relatively simple Magnetisation Transfer Ratio (MTR) to the rate constants and volume fractions of the different tissue compartments involved), diffusion parameters (including diffusivity and anisotropy), flow and perfusion. While details will of course be study dependant, we will consider examples of T_1 & T_2 , MTR & qMT and DTI measurement methods, looking for hints and 'rules of thumb' applicable to any quantitative study. In particular, we will aim to show that:

- Acquisition and processing must be considered together
- Models used in processing must be appropriate
 - two models may give different answers
 - may both be 'correct' (in certain circumstances)

- Both accuracy (how close the answer is to the ‘correct’ value) and precision (how reproducible the answer is) should be considered
- Effect of noise (& noise propagation) must be understood

Relaxation Times

The relaxation times T_1 , T_2 , T_2^* describe the behaviour of the magnetization in an NMR experiment. They are tissue specific, being related to chemical structure and composition of environment and are responsible (along with proton density) for the majority of contrast seen in conventional MR images.

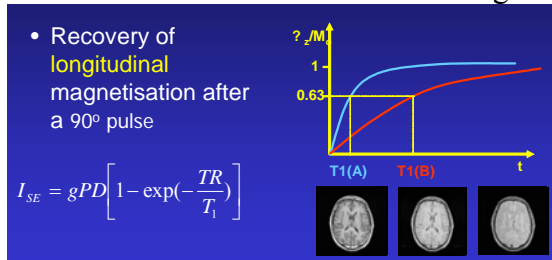


Figure 2

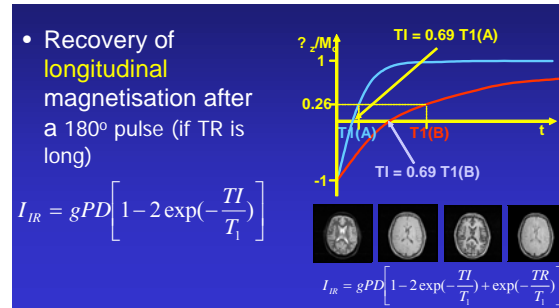


Figure 1

T_1 - the Longitudinal or Spin-lattice relaxation time - is the time constant for recovery of longitudinal magnetisation after perturbation (Fig1 & 2).

T_2 - the Transverse or Spin-spin relaxation time - is the time constant for decay of the transverse magnetisation after an RF pulse in a homogenous static magnetic field (Fig 3); T_2^* is the time constant for the same decay in an inhomogeneous field.

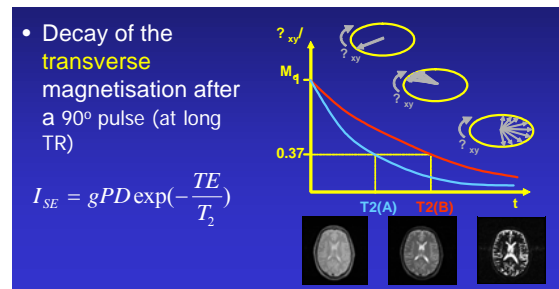


Figure 3

T_1 Measurement

T_1 can be calculated (on a pixel by pixel basis) by curve fitting to measurements from multiple inversion times or multiple saturation times, using a sequence with a short TE spin echo readout, although the formulae for the inversion recovery become complex unless long TRs are used, leading to very long scan times. The long scan times mean a potential for movement between scans, but the methods both have good reproducibility and accuracy.

T_1 can also be computed by directly comparing signal intensity of short and very long TR sequence:

$$T_1 = \frac{TR}{\ln\left(1 - \left(\frac{I_{SE_1}}{I_{SE_2}}\right)\right)}$$

This two point method is relatively fast, although there is still a potential for movement between the scans. It has reasonable reproducibility, but accuracy is poor.

A number of much quicker T_1 measurement methods have also been reported, based on FLASH, (eg⁽¹⁾), EPI, (eg^{(2), (3)}) and Look-Locker methods (which sample the recovering magnetisation several times after a single inversion pulse (eg^{(4), (5)})). Methods are also available that use SSFP (eg DESPOT1 and DESPOT2^{(6), (7)}, see Fig 4, below). Multi inversion recover remains the ‘gold standard’, however, and while other sequences offer faster acquisition and better coverage, they usually have lower accuracy, and assume a single T_1 value (which is generally appropriate in areas of uniform tissue, but can cause problems in areas of ‘partial volume’ between tissues, particularly near CSF (Cerebro-Spinal Fluid) spaces as CSF has a very different T_1 value from white and grey matter).

T_2 Measurement

T_2 can be calculated (on a pixel by pixel basis) by curve fitting to spin echo measurements from multiple echo times (at long TR). The measurements can be from multiple single echo acquisitions, but this is extremely time consuming, with a high likelihood of movement between scans. The effects of diffusion also vary between the acquisitions, potentially confounding the measurement and reducing accuracy. The diffusion confound can be reduced, the scan time shortened, and the possibility of mis-registration between images removed, by using a multi-echo sequence to collect all TE values in a single acquisition. Such a sequence (often referred to as a CPMG (Carr-Purcell-Meiboom-Gill) acquisition) has high accuracy and precision, but requires extremely accurate 180° refocusing pulses, and can therefore only be implemented in a single slice mode, using ‘hard’ pulses, making it extremely inefficient.

T_2 can also be computed by directly comparing directly comparing signal intensity of two sequences with different TEs:

$$T_2 = \frac{TE_2 - TE_1}{\ln(I_{SE_1} / I_{SE_2})}$$

This two point method can be implemented by collecting two separate echoes (with the potential for motion between scans), or as a dual echo sequence (sacrificing some accuracy unless a calibration is performed⁽⁸⁾). Both versions have reasonable reproducibility, but do not approach the accuracy of the CPMG sequence.

T_2 decay can show non-single exponential behaviour, even in the absence of gross partial volume effects as there are multiple compartments within tissue which have different T_2 values. Partial volume effects are an addition problem, particularly near CSF spaces as CSF has a very different T_2 value from white and grey matter. The multiple components can be differentiated by a multi echo sequence; this can be used either to reduce/remove contamination from an unwanted tissue (eg⁽⁹⁾), or, by using non-negative least squares (NNLS) to fit spectrum of T_2 values from a large number of echoes (≥ 32) to visualise the very short T_2 component (≤ 20 ms) thought to represent water trapped between myelin bi-layers⁽¹⁰⁾⁽¹¹⁾⁽¹²⁾.

A number of much quicker T_2 measurement methods have also been reported, based on FLASH, (eg⁽¹³⁾⁽¹⁴⁾⁽¹⁵⁾), EPI, (eg⁽¹⁶⁾). Methods are also available that use SSFP (eg DESPOT1 and DESPOT2).

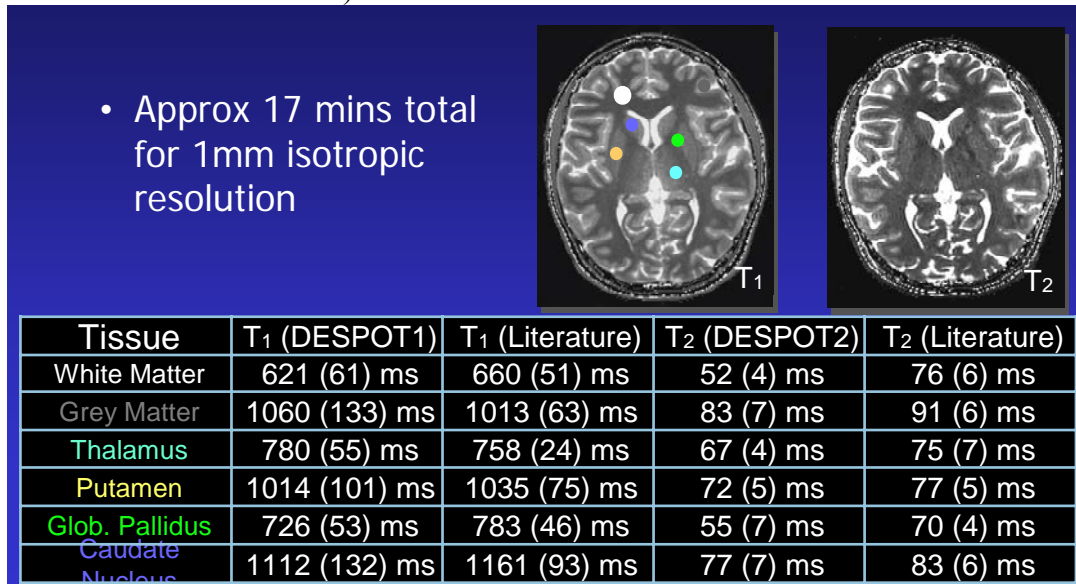


Figure 4 – T₁ and T₂ maps from DESPOT1 & DESPOT2

Multi-echo CPMG recover remains the ‘gold standard’, and, as with T₁ measurement, while other sequences offer faster acquisition and better coverage, they usually have lower accuracy, and assume a single T₂ value. Fast spin echo based sequences (which, like CPMG, may reduce the confounds of diffusion) and fast-FLAIR sequences (which minimize contamination from the very long T₂ of CSF) are available and have been shown to have good reproducibility⁽¹⁷⁾, although their use can be controversial⁽¹⁸⁾⁽¹⁹⁾⁽²⁰⁾.

Magnetisation Transfer

In many tissues there are two (or more) distinct water compartments (Fig 5). Magnetisation transfer sequences use the ‘free water’ (which has a relatively long T₂ (~50ms) and narrow line in a

- Free water
 - produces normal MR signal
 - relatively long T₂ (~50ms)
 - narrow line in spectrum (~20Hz)
- Bound water
 - ‘invisible’ on normal MRI
 - very short T₂ (<100us)
 - very wide line in spectrum (>10kHz)

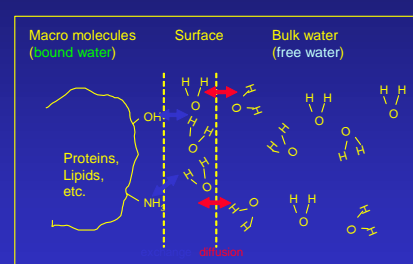


Figure 5

proton spectrum (~20Hz), and produces normal MR signal) to probe the ‘bound water’, which is invisible on normal MRI because of its very short T₂ (<100us) (and correspondingly very wide line in a spectrum (>10kHz)). Off-resonance saturation can

irradiate the bound pool without directly affecting free pool, leading to a change in the latter's signal intensity (and T1) in areas where MT occurs.

Henkelmann's two pool model⁽²¹⁾ can predict the signal intensity given the frequency and power of the MT pulse. Ramani et al⁽²²⁾ (and others) have shown that it is possible to modify the model to allow for the pulsed saturation used in typical in vivo experiments, and by collecting a relatively small number of images to

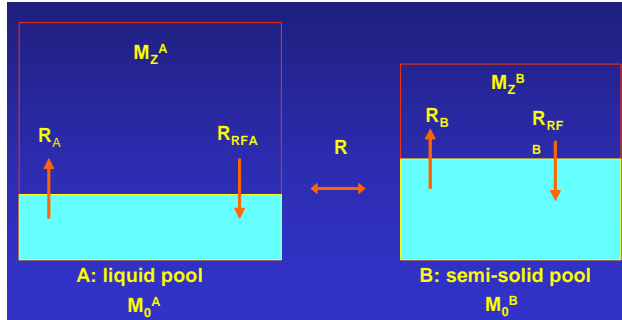


Figure 6

$$S^A = g M_Z^A = g M_0^A \left(\frac{R_B \left[\frac{RM_0^B}{R_A} \right] + R_{RFB} + R_B + RM_0^A}{\left[\frac{RM_0^B}{R_A} \right] (R_B + R_{RFB}) + \left(1 + \left[\frac{\omega_{CWPE}}{2\pi\Delta f} \right]^2 \left[\frac{1}{R_A T_2^A} \right] \right) (R_{RFB} + R_B + RM_0^A)} \right)$$

$$R_{RFA} = \frac{\omega_1^2 T_2^A}{1 + (2\pi\Delta f T_2^A)^2} \quad \text{and} \quad R_{RFB} = \omega_1^2 \sqrt{\frac{\pi}{2}} T_2^B e^{-\frac{(2\pi\Delta f T_2^B)^2}{2}}$$

$$\omega_{CWPE} = \gamma B_{ICWPE} \quad B_{ICWPE} = \sqrt{P_{SAT}} = \sqrt{\frac{1}{TR'} \int_0^{\tau_s} B_1^2(t) dt}$$

Figure 7

extract physically meaningful, quantitative, parameters, which are not pulse sequence or irradiation dependant. From 6 or more MR images, five independent quantities - R^B , RM_0^B/R^A , R , $1/R^A T_2^A$ and T_2^B - can be calculated (Fig 7) and, with a separate measurement of T_1 (T_{1obs}), the bound water fraction, f , (thought to represent myelin content) can be found.

MT is a good example of the compromises often required, however, as due to scan time limitations, it is more common to measure:

- Magnetisation Transfer Ratio (MTR)
 - Needs collection of only 2 images
 - NOT a physically meaningful parameter
 - pulse sequence and irradiation dependant
 - but related to tissue structure
- 'forward rate constant'
 - Needs collection of only 3 images
 - physically meaningful parameter, but assumes complete saturation
 - (impossible to achieve in humans!)
 - related to tissue structure

$$MTR = \frac{100 \cdot (S_u - S_s)}{S_u}$$

$$k_f = \left(\frac{1}{T_{1sat}} \right) \left(1 - \frac{S_s}{S_u} \right)$$

Diffusion

Diffusion is the random translational motion of molecules (water). In a test tube diffusion is largely unhindered (free) and isotropic, and is characterised by the diffusion constant; in the brain it is *restricted* or *hindered*, and is characterised by the *apparent diffusion*

coefficient (ADC). In the brain diffusion may be anisotropic, as barriers to diffusion (e.g. axon walls, cellular microstructures) are oriented, so diffusion is characterised by different ADCs in different directions.

Any MR sequence can be sensitized to diffusion by adding gradients, although for efficiency, and to minimize sensitivity to bulk motion, EPI based sequences are often used. The fullest (simple) description of diffusion is given by the diffusion tensor:

$$\mathbf{D} = \begin{pmatrix} D_{xx} & D_{xy} & D_{xz} \\ D_{yx} & D_{yy} & D_{yz} \\ D_{zx} & D_{zy} & D_{zz} \end{pmatrix}$$

The tensor can be calculated from 6 (or more) measurements with sensitizing gradients in different directions, and can be diagonalised to give eigenvectors, representing the principle directions of diffusion and eigenvalues, λ_1 , λ_2 , λ_3 representing the magnitude of diffusion. From the tensor, various rotational invariant parameters can be calculated including mean diffusivity and fractional anisotropy (FA) (Fig 8).

The quality of the final images is highly dependant on number of averages, and the b-values chosen, with collection of more than the minimum 6 required directions improving the SNR by more than would be achieved by averaging in the same scan time. The optimum protocol depends on what is to be measured (eg single direction ADC, tensor for FA, etc ...) ⁽²³⁾⁽²⁴⁾, and, as with MTR, compromises must often be made.

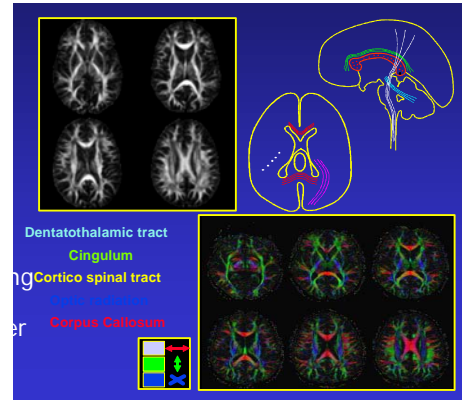


Figure 8

Alternative Diffusion Models

The tensor is only one model of diffusion. Experiments have been performed showing non-monoexponential decay ⁽²⁵⁾⁽²⁶⁾, and very different ADC and FA values are found depending on the b-value used (Fig 9). Areas where multiple fibres can be detected have also been shown, and to allow

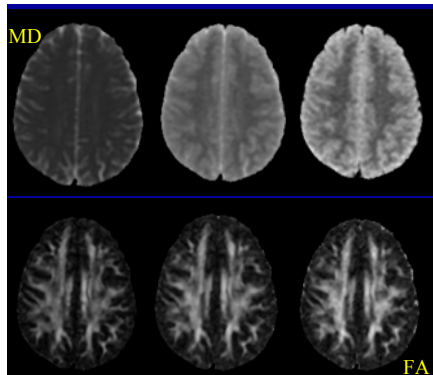


Figure 10 quantification in these cases, models other than the diffusion tensor have been devised including q-space (or more practical approximations ⁽²⁷⁾), PAS-MRI ⁽²⁸⁾, and others; Fig 10 shows an

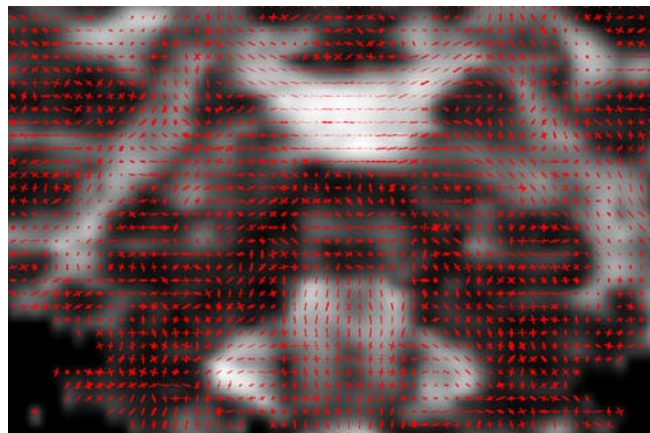


Figure 9

example of the (multiple) principle directions of diffusion seen in the pons by PAS-MRI.

Noise in Magnitude Images

Noise in magnitude images follows a Ricean Distribution (Fig 9), which tends to a Gaussian Distribution at high signal and a Rayleigh Distribution at low intensity. The background noise has a non-zero mean (mean = 1.253σ ; s.d. = 0.655σ , where σ is ‘true’ standard deviation of the noise in real (or imaginary) data)⁽²⁹⁾. This means that at low values (as often occur in diffusion, and other quantitative measurements) the intensity of images are artificially increased, and this must be allowed for in any fitting procedure (eg by fitting to the square of the image intensity⁽³⁰⁾).

General Suggestions for Quantitative Mapping

Similar trade off occurs when measuring most parameters; multi point methods are slow but accurate (and accurate over a range of values), while two point methods are faster, but inherently assume single component to decay and are accurate only over a limited range. When setting up a quantitative measurement protocol (for any measure), the size of feature to be measured must first be considered, as this will determine field of view, matrix size, slice thickness, etc. The available scan time then determines the total number of images that can be obtained (with these parameters), which in turn determines which model(s) can be used. (Remember that all models have assumptions, and results are only meaningful if these assumptions are met). If, as is often the case, as two point measurement must be made, then the echo times (for TE measurements) should be spaced to cover the expected T_2 value or ranges (with one as short as possible and one at, or just above, the expected T_2); the TRs, for T_1 measurement and b values for ADC measurement follow similar principles. As many averages as scan time allows should be collected, and these should be distributed in proportion to give both (all) images similar final SNR (for single component decays (T_1 , T_2 , ADC ...), extra points on a decay curve are less useful than extra averages of points at the extremes).

Finally, always run a pilot set of scans and check the results look ‘reasonable’ and also always check scan-rescan reliability!

Acknowledgements

Sean Deoni, Anita Ramani, Paul Tofts, Claudia Wheeler-Kingshott, Derek Jones, Mara Cercignani, Geoff Parker, Danny Alexander, and anyone else who un-wittingly provided data!

References

-
- (1) Bluml S., Schad L.R., Boris S., Lorenz W.J. Spin-lattice relaxation time measurement by means of a TurboFLASH technique. *Magn. Reson. Med.* 1993; 30:289-295.
 - (2) Ordidge, R.J., Gibbs, P., Chapman, B., Stehling, M.K., Mansfield, P. High-speed multislice T_1 mapping using inversion-recovery echo-planar imaging. *Magn. Reson. Med.* 1990; 16:238 –245.
 - (3) Clare S, Jezzard P. Rapid T_1 mapping using multislice echo planar imaging. *Magn. Reson. Med.* 2001; 45:630-4.
 - (4) Brix G., Schad L.R., Deimling M., Lorenz W.J. Fast and precise T_1 imaging using a TOMROP sequence. *Magn. Reson. Imag.* 1990; 8:351-356.

-
- (5) Henderson E., McKinnon G., Lee T.Y., Rutt B.K. A fast 3D Look-Locker method for volumetric T₁ mapping. *Magn. Reson. Imag.* 1999; 17:1163-1171.
- (6) Deoni S.C.L., Rutt B.K., Peters T.M. Rapid combined T₁ and T₂ mapping using gradient recalled acquisition in the steady state. *Magn. Reson. Med* 2003; 49:515-526.
- (7) Deoni S.C., Peters T.M., Rutt B.K. High-resolution T₁ and T₂ mapping of the brain in a clinically acceptable time with DESPOT1 and DESPOT2. *Magn. Reson. Med.* 2005; 53:237-41.
- (8) G.J. Barker G.J., Parker G.J.M. and Tofts P.S., Accurate T₂ Measurement using Dual Echo Spin Echoes, Proceedings of the European Society of Magnetic Resonance in Medicine and Biology 16th Annual Meeting, 1999, Seville, 510.
- (9) Thorpe J.W., Barker G.J., Jones S.J., Moseley I., Losseff N., MacManus D.G., Webb S., Mortimer C., Plummer D.L., Tofts P.S., McDonald W.I. and Miller D.H., Magnetisation Transfer Ratios and Transverse Magnetisation Decay Curves in Optic Neuritis: Correlation with Clinical Findings and Electrophysiology, *JNNP*, 1995, 59, 487-492.
- (10) MacKay A., Whittall K., Adler J., Li D., Paty D., Graeb D. In vivo visualization of myelin water in brain by magnetic resonance. *Magn. Reson. Med.*;31:673-7
- (11) Whittall K.P., MacKay A.L., Graeb D.A., Nugent R.A., Li D.K., Paty D.W. In vivo measurement of T₂ distributions and water contents in normal human brain. *Magn. Reson. Med.* 1997;37:34-43.
- (12) Jones C.K., Whittall K.P., MacKay A.L. Robust myelin water quantification: averaging vs. spatial filtering. *Magn. Reson. Med.* 2003;50(1):206-9.
- (13) Haase, A. SNAPSHOT FLASH MRI. Applications to T₁, T₂, and chemical-shift imaging. *Magn. Reson. Med.* 1990; 13:77.
- (14) Deichmann R., Haase A. Quantification of T₂ values by Snapshot-FLASH NMR Imaging. *J. Magn. Reson.* 1992; 96:608.
- (15) Deichmann R., Adolf H., Noth U., Morrissey S., Schwarzbauer C., Haase A. Fast T₂-mapping with SNAPSHOT FLASH imaging. *Magn Reson Imag* 1995; 13: 633-639.
- (16) McKenzie C.A., Chen Z., Drost D.J., Prato F.S. Fast acquisition of quantitative T₂ Maps. *Magn Reson Med* 1999; 41: 208-212
- (17) Melhem E.R., Whitehead R.E., Bert R.J., Caruthers S.D. MR imaging of the hippocampus: measurement of T₂ with four dual-echo techniques. *Radiology.* 1998;209:551-5.
- (18) Duncan J.S., Bartlett P., Barker G.J. Technique for measuring hippocampal T₂ relaxation time. *AJNR Am J Neuroradiol.* 1996;17:1805-10.
- (19) Jack C.R. Jr. Hippocampal T₂ relaxometry in epilepsy: past, present, and future. *AJNR Am J Neuroradiol.* 1996;17:1811-4.
- (20) Duncan J.S., Bartlett P., Barker G.J. Measurement of hippocampal T₂ in epilepsy. *AJNR Am J Neuroradiol.* 1997;18:1791-2.
- (21) Henkelman R.M., Huang X., Xiang Q.S., Stanisz G.J., Swanson S.D., Bronskill M.J. Quantitative interpretation of magnetization transfer. *Magn. Reson. Med.* 1993;29:759-66.
- (22) Ramani A., Dalton C., Miller D.H., Tofts P.S., Barker G.J. Precise estimate of fundamental in-vivo MT parameters in human brain in clinically feasible times. *Magn. Reson. Imaging.* 2000;20:721-31.
- (23) Jones DK, Horsfield MA, Simmons A. Optimal strategies for measuring diffusion in anisotropic systems by magnetic resonance imaging. *Magn Reson Med.* 1999;42:515-25.
- (24) Alexander DC, Barker GJ. Optimal imaging parameters for fiber-orientation estimation in diffusion MRI. *Neuroimage.* 2005;27:357-67.
- (25) Clark C.A., Le Bihan D. Water diffusion compartmentation and anisotropy at high b values in the human brain. *Magn. Reson. Med.* 2000;44:852-9.
- (26) Clark C.A., Hedehus M., Moseley M.E. In vivo mapping of the fast and slow diffusion tensors in human brain. *Magn Reson Med.* 2002;47:623-8.
- (27) Tuch D.S., Reese T.G., Wiegell M.R., Wedeen V.J. Diffusion MRI of complex neural architecture. *Neuron.* 2003;40:885-95.
- (28) Jansons K.M., Alexander D.C. Persistent Angular Structure: new insights from diffusion MRI data. *Inf Process Med Imaging.* 2003;18:672-83.
- (29) Henkelman R.M. Measurement of signal intensities in the presence of noise in MR images. *Med Phys.* 1985;12:232-3. Erratum in: *Med Phys.* 1986;13:544.
- (30) Miller A.J., Joseph P.M. The use of power images to perform quantitative analysis on low SNR MR images. *Magn Reson Imaging.* 1993;11:1051-6.